the other group was the carrageenan-treated group (PbCGN group). Another group of uninfected mice was also treated with λ-carrageenan (CGN group). λ-carrageenan (SIGMA) was dissolved in PBS (2 mg/ml) at 65°C and passed through a 0.45-μm filter (Millipore) for sterilization prior to use. λ-carrageenan was given intraperitoneally at a dose of 25 mg/kg BW following the four-day suppressive test. In this protocol, the infection day is designated as day 0. The first treatment is given 2 h after infection, and then subsequent treatments are given every 24 h until day 3 post-infection, for a total of four treatments.

To determine the survival rate, half of the infected mice in each group were observed for clinical signs of cerebral malaria until the mice eventually succumbed to the disease. The other half of each group was sacrificed under terminal isoflurane anesthesia at the presumed onset of cerebral malaria for histopathological examination and Evans blue dye assays.

Parasitaemia, ECM signs, and survival monitoring

Parasitaemia levels of both groups of infected mice (n = 4) were monitored from days 4 to 10 post-infection by using Giemsa-stained thin blood smears. Ten oil immersion objective fields were examined each with 200–300 red blood cells. The infected mice were observed for general signs of malaria such as ruffled fur, and hunching posture, and for ECM-related signs such as wobbly gait, head tilt, limb paralysis, convulsions, and coma. Other behavioural parameters monitored included reactions to stimuli such as exploration of a new environment and touch reflexes [15,16]. Deaths were promptly recorded.

Histopathology, intracerebral haemorrhage scoring, and statistical analysis

The infected mice were sacrificed under terminal isoflurane anesthesia once the clinical signs of ECM were observed in some or all members of the treatment groups. This corresponded to day 5 p.i. in all members of the PbCGN group (n = 4). Although no signs of CM were observed, the PbN mice (n = 4) were also sacrificed at this time. Normal and healthy mice (N, n = 4) and uninfected, carrageenan-treated mice (CGN, n = 4) were also sacrificed at the same time for comparison. Brains as well as other vital organs including kidneys, livers, hearts, lungs, and spleens were collected and fixed in 4% paraformaldehyde and embedded in paraffin. The organs were sectioned at 5 μm and were stained with haematoxylin-eosin (HE) stain. The brain sections were examined for haemorrhages and inflammation. Intracerebral haemorrhages were recorded [16]. Statistically significant differences in the number of intracerebral haemorrhages were determined by using the Mann–Whitney U test. Values were considered to be significantly different when the P value was less than 0.05. The organ sections were examined for any significant lesions.

Assessment of vascular leakage at the blood–brain barrier by use of Evans blue dye perfusion

On day 5 post-infection, 200 μl of 1% Evans blue dye was injected into the tail veins of representative mice (n = 3–4) from each treatment group. After 1 h, the mice were sacrificed and their brains were collected and examined for bluish discoloration. The brains were then placed in 4% paraformaldehyde for 48 h to extract the Evans blue dye, and the absorbance was measured at a wavelength of 600 nm [15]. For this, the results of two independent assays were pooled. Absorbance readings were carried out in triplicates and the mean of three replicates was computed. Statistically significant differences in the absorbance of Evans blue dye between the groups were determined by using Tukey's multiple comparison test. Values were considered to be significantly different when the P value was less than 0.05.

Results

Effects of λ-carrageenan treatment on parasitaemia and course of infection

Lambda-carrageenan poorly inhibited the growth of *P. berghei* ANKA, as shown by the hyperparasitaemia in the infected mice (Figure 1A), and did not improve the survival of the infected mice (Figure 1B). These findings differ from the report by James and Alger [2], who found that A/J Swiss mice infected with *P. berghei* NK65 survived for up to 28 days when pre-treated with calcium carrageenan intraperitoneally, and from the finding of Adams that λ-carrageenan effectively inhibited the growth and invasion of red blood cells by *P. falciparum* in *in vitro* experiments [1].

In the experiments monitoring parasitaemia, ECM, and survival, all *P. berghei* ANKA-infected mice exhibited signs of ruffled fur, hunching, and decreased reaction to stimuli on day 5 post-infection. PbCGN mice showed limb paralysis, convulsions, head tilt, and coma and died soon afterwards. On the same day, PbN mice showed none of these neurological signs. Deaths in the PbN mice group were first seen on day 7 p.i and all of the PbN mice died by day 13 p.i. Signs observed in the PbN mice that started to die from day 7 until day 13 p.i. included general weakness and lethargy, while signs that are related to ECM, specifically, limb paralysis, convulsions, and head tilt were not seen.

Gross pathology and histopathology of the brains of *Plasmodium berghei*-infected BALB/c mice

Haemorrhages were visible on the brains of the PbCGN mice that showed clinical signs of CM and were sacrificed on day 5 p.i. (n = 4) (Figure 2A). Similarly, haemorrhages were also observed in the PbN mice that were sacrificed

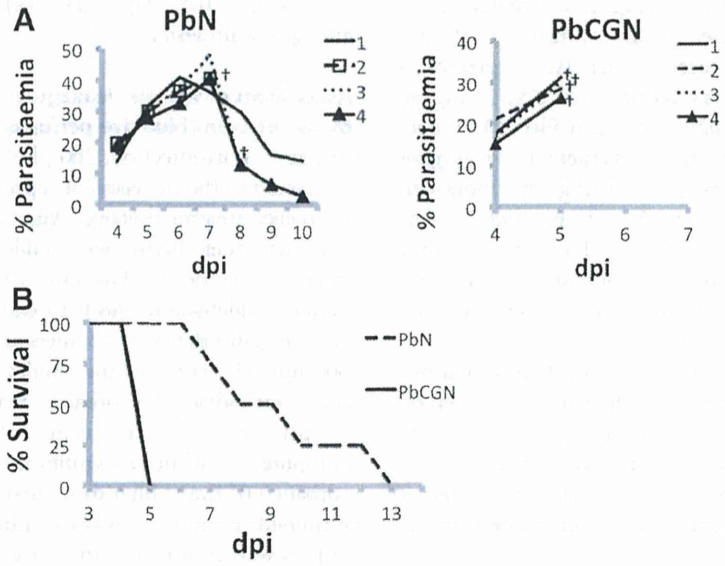

Figure 1 Parasitaemia and survival profiles of *P. berghei* ANKA-infected BALB/c mice. (A) Four mice per group were infected with *P. berghei* ANKA, and were not treated (PbN) or treated with λ-carrageenan (PbCGN). The parasitaemia in the blood microvessels is shown for each animal per group (n = 4). λ-carrageenan treatment (25 mg/kg) did not inhibit the growth of *P. berghei* ANKA *in vivo* using the four-day suppressive test. The dagger (†) indicates mouse death. **(B)** Survival profiles of *P. berghei* ANKA-infected BALB/c mice: λ-carrageenan-treated (PbCGN); not treated (PbN).

on the same day (n = 4) (Figure 2B). These PbN mice, however, did not necessarily show neurological signs related to cerebral malaria. This result shows that in the BALB/c mouse, which is considered to be resistant to the development of CM by *P. berghei* ANKA infection, in the absence of clear neurological signs, haemorrhagic brain lesions can be observed.

To further characterize the lesions in the brains of mice infected with *P. berghei* ANKA and then treated with λ-carrageenan, two independent experiments for histopathological examinations were done with similar observations. No apparent lesions were observed in the brain sections of uninfected, healthy carrageenan-treated mice (CGN group, Figure 3A). By contrast, microthrombi, intracerebral haemorrhages, and the presence of iRBCs in brain vessels were observed in both PbN (as shown in Figure 3B) and PbCGN (Figure 3C and D) animals. Perivascular infiltrations of inflammatory cells around the microthrombi were also observed in the PbCGN group and not as much in the PbN group. In addition, hyperplastic endothelium of brain blood vessels was observed only in the PbCGN group (Figure 3C and D). These results indicate that the administration of λ-carrageenan to BALB/c mice infected with *P. berghei* ANKA caused more severe histopathological features associated with cerebral malaria.

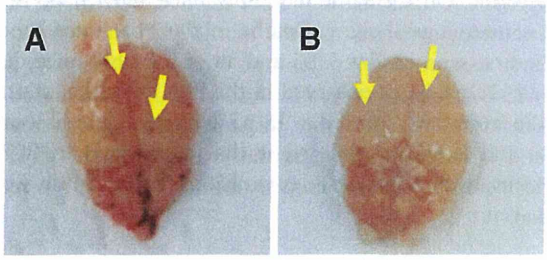

Figure 2 Gross lesions on the brains of infected mice. (A) From PbCGN mice that were sacrificed at the presumed onset of cerebral malaria 5 days p.i. showing clinical signs such as head tilting and convulsions. **(B)** From a Pb-infected, untreated (PbN) mouse sacrificed on day 5 p.i. that did not show any signs associated with CM. Yellow arrows show petechial haemorrhages.

Histopathology of other vital organs revealed malaria pigment deposits in lung sections and in the Kupffer cells in the livers of both the PbN and PbCGN groups. The presence of necrotized lymphocytes and follicular hyperplasia was also observed in the spleens of both infected groups. No apparent lesions were observed in the kidneys or hearts of these infected mice. These results show that λ-carrageenan treatment had no atypical effects on the other vital organs of the *P. berghei*-infected BALB/c mice.

Intracerebral haemorrhage counts

Intracerebral haemorrhages observed in sections from four major regions of the brain, namely, the frontal lobe, diencephalon, occipital lobe, and cerebellum, were counted and tallied (n = 4, PbN and PbCGN, respectively). There were no statistically significant differences

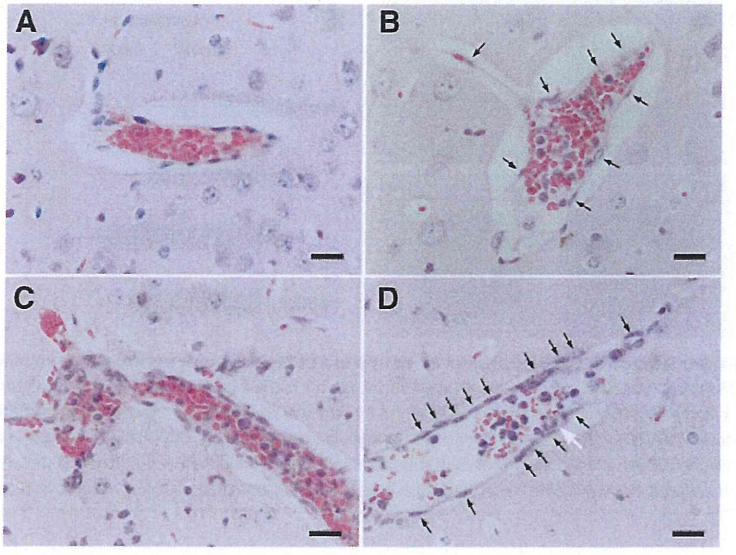

Figure 3 Brain histopathology. (A) CGN group. No apparent lesions are observed (Haematoxylin-Eosin stain). Bar, 20 μm. **(B)** PbN group. Microthrombus consisting of fibrin pigmented RBCs and accumulated mononuclear cells, is observed. Perivascular infiltration of inflammatory cells is not observed. Vascular endothelium is not hyperplastic (arrows indicate endothelial cells). Bar, 20 μm. **(C)** PbCGN group. Microthrombus consisting of fibrin, pigmented RBCs, pigmented macrophages, and mononuclear cells is observed. Perivascular infiltration of inflammatory cells, haemorrhage in perivascular space, and hyperplastic vascular endothelium are also observed. Bar, 20 μm. **(D)** PbCGN group. Infected RBCs and inflammatory cells can be seen within the blood vessels of the cerebrum. Note the hyperplastic endothelium, characterized by increased number of endothelial cells (arrow). Adhesive Pb-laden macrophages (shown by white arrow) can also be seen. Bar, 20 μm.

in the number of intracerebral haemorrhages between the PbN and PbCGN groups. However, haemorrhages were observed in all regions of the brains of all of the PbCGN mice, whereas they were observed in only half of the PbN mice tested (Table 1). These findings are consistent with the increased severity of the pathology in the PbCGN mice relative to the PbN mice.

Assessment of vascular leakage at the blood–brain barrier by using Evans blue dye perfusion

To further evaluate the effects of λ-carrageenan on the integrity of blood–brain barrier (BBB), and its contribution to the early death of the mice infected with *P. berghei* ANKA, the permeability of the blood–brain barrier was assessed by using Evans blue assay. Representative images of the brains of mice from each group are shown in Figure 4. The brains of the PbN and PbCGN mice (Figure 4C and D, respectively) absorbed the dye, indicating increased permeability of the blood–brain barrier compared with that of the brains of normal mice and CGN mice (Figure 4A and B, respectively). As expected, CGN mice showed increased levels of blood–brain barrier leakage relative to the levels in the brains of normal mice. However, there were no statistically significant differences in the levels of Evans blue dye leakage from the mouse brains between the PbN and PbCGN groups (Figure 4E). These results indicate that not only the altered integrity of blood–brain barrier but also other factors may lead to this severe complication of malaria in mice infected with *P. berghei* ANKA.

Table 1 Intracerebral haemorrhage counts

Haemorrhage score	PbN				PbCGN				Mann–Whitney *P*
	A	B	C	D	E	F	G	H	
Frontal Lobe	2	0	0	4	6	4	9	3	0.05755
Diencephalon	5	0	0	1	6	4	9	3	0.1059
Occipital Lobe	4	2	0	6	2	4	7	2	0.6552
Cerebellum	5	0	0	1	4	6	4	4	0.1367
Total	16	2	0	12	14	19	27	11	0.1489

Statistically significant differences in intracerebral haemorrhage counts were determined by using the Mann–Whitney test. Values were considered to be significantly different when the *P* value was less than 0.05.

Discussion

Here, the *in vivo* efficacy and safety of λ-carrageenan as an anti-malarial drug was evaluated. The results show that λ-carrageenan poorly inhibited the growth of *P. berghei* ANKA in BALB/c mice and caused more severe brain lesions, leading to the early death of the mice. BALB/c mice, which are considered to be relatively resistant to the consequences of cerebral malaria caused by the ANKA strain of *P. berghei* [10,17-19], were chosen as model to assess the effects of the administration of λ-carrageenan to the development of clinical signs associated with cerebral malaria. Both groups were shown to develop a high parasitaemia, but the

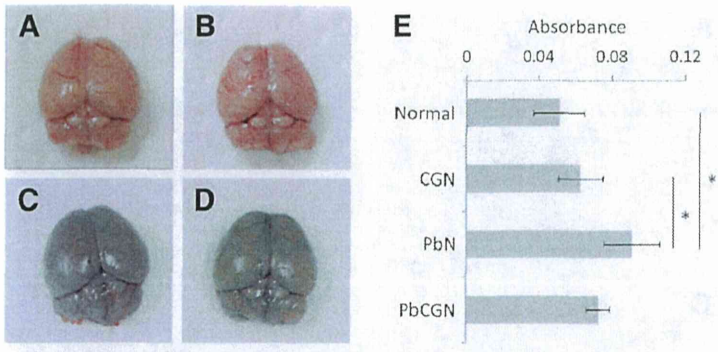

Figure 4 Assessment of vascular leakage at the blood–brain barrier by use of Evans blue dye perfusion. Two hundred microliters of 1% Evans blue dye was injected into the tail veins of each mice on day 5 post-infection. After 1 h, the mice were sacrificed using terminal isoflurane anesthesia and the brains were collected. Representative brains are shown: **(A)** Normal healthy mouse (N), **(B)** Carrageenan-treated mouse (CGN), **(C)** *P. berghei* ANKA-infected, untreated mouse (PbN), **(D)** *P. berghei* ANKA-infected, carrageenan-treated mouse (PbCGN). **(E)** The mean absorbances at 600 nm wavelength and standard deviations of extracted dye after placing the brains in 4% paraformaldehyde for 48 h are shown for each group. Statistically significant differences in mean absorbances were determined by using Tukey's multiple comparison test (*: *P* value < 0.05, ns: not significant).

infected BALB/c mice treated with λ –carrageenan showed more signs related to ECM and died earlier than the untreated mice. The attempts to show that λ-carrageenan treatment could cause more severe cerebral malaria through histopathology and Evans blue dye assays revealed almost the same results for both groups of infected mice. The levels of blood–brain barrier leakage were similar between the *P. berghei*-infected mice that were mock-treated and those that were administered λ-carrageenan; and the histopathological findings on the brains show the presence of intracranial haemorrhages for both groups. It is important to note that with the small sample size used in this study, the statistical data presented here should be interpreted with caution [20-22].

It is also possible that although the clinical signs associated with ECM in the untreated group were not observed, these mice may also have developed ECM, as reported by Neill and Hunt [23]. It will be interesting to explore the underlying mechanisms as to why clear neurological signs were not as evident in the untreated group given that there was hyperparasitaemia, leakage in the BBB and presence of intracranial haemorrhages. These results indicate that there may be other factors involved in the early death of mice treated with λ-carrageenan during *P. berghei* ANKA infection. One can also consider the possibility that the hyperplastic endothelium of the brain blood vessels compensated for the blood–brain barrier leakage in the PbCGN group.

Lambda-carrageenan is known to induce inflammatory pain and to alter the permeability of the blood–brain barrier in several animal models [9,24]. Moreover, administration of λ-carrageenan increases the expression of ICAM-1, which plays a key role in the sequestration of iRBCs in cerebral malaria under experimental and natural conditions [25,26].

By contrast, λ-carrageenan is known to activate the innate immunity that depends on Toll-like receptor 4 (TLR4) and Myd88 [5]. Given that the activation of TLR4/Myd88 signaling causes acute inflammatory injury [27], one could argue that the early deaths of mice treated with λ-carrageenan during the *P. berghei* ANKA infection could be attributed to the dysregulation of innate immunity rather than the dysfunction of the blood–brain barrier. Further studies are warranted to elucidate the molecular basis of this exacerbation of pathology.

Malaria remains a threat to human health and there is an urgent need to develop and test novel compounds. The results presented here suggest that λ-carrageenan, a sulphated polysaccharide which is a common food additive and ingredient in household products and has been found to inhibit the invasion of red blood cells by malaria merozoites *in vitro*, may be unsuitable for the treatment of clinical malaria.

However, other sulphated polysaccharides, including heparin, fucoidan, and dextran sulfate [28,29] have shown promising *in vitro* anti-malarial activity. An example is the previous report on gellan sulfate [30] that demonstrated that chemical modification, namely, sulphation, could change the characteristics of these compounds. Given that these polysaccharides are still considered promising potential anti-malaria drugs, chemical modification might decrease the side effects of such compounds.

Conclusion

This study shows the potential toxicity of λ-carrageenan as an antimalarial using the BALB/c mice as model of

ECM. We find the usefulness of this rodent model in elucidating CM pathogenesis and evaluating promising antimalarial candidates *in vivo* and more importantly the safety profile of anti-malarial compounds that could not be envisaged if only *in vitro* experiments were conducted.

Abbreviations

CM: Cerebral malaria; ECM: Experimental cerebral malaria; HCM: Human cerebral malaria; BBB: Blood–brain barrier; iRBCs: Infected red blood cells; H-E: Haematoxylin-eosin stain.

Competing interests

The authors declare that they have no competing interests.

Authors' contributions

FCR and KK designed the study. FCR performed all of the animal experiments and wrote the manuscript. RT conducted the statistical studies and co-wrote the manuscript. SC, NH, and YK prepared the histopathology slides and performed all of the histopathological examinations. TS, HT, FM, A. Ishiwa, A. Inomata, and TH contributed to the data analysis. KK edited the manuscript and supervised the study. All authors have read and approved the final version of the manuscript.

Acknowledgements

This study was supported by Grants-in-Aids for Young Scientists, and Scientific Research on Innovative Areas (3308) from the Ministry of Education, Culture, Science, Sports, and Technology (MEXT) and for Research on global health issues from the Ministry of Health, Labour, and Welfare of Japan, by Bio-oriented Technology Research Advancement Institution (BRAIN), by the Naito Foundation, and by the Programme to Disseminate Tenure Tracking System from the Japan Science and Technology Agency (JST).
We would also like to thank Dr. Maria Shirley Herbas of the NRCPD, Obihiro University of Agriculture and Veterinary Medicine for providing training on tissue handling and collection.

Author details

[1]Department of Veterinary Microbiology, Graduate School of Agricultural and Life Sciences, The University of Tokyo, 1-1-1 Yayoi, Bunkyo-ku, Tokyo 113-8657, Japan. [2]National Research Center for Protozoan Diseases, Obihiro University of Agriculture and Veterinary Medicine, Obihiro 080-8555, Hokkaido, Japan. [3]Department of Basic Veterinary Medicine, Obihiro University of Agriculture and Veterinary Medicine, Obihiro 080-8555, Hokkaido, Japan. [4]Department of Veterinary Paraclinical Sciences, College of Veterinary Medicine, University of the Philippines Los Baños, Laguna 4031, Philippines.

Received: 1 September 2014 Accepted: 7 December 2014
Published: 11 December 2014

References

1. Adams Y, Smith SL, Schwartz-Albiez R, Andrews KT: **Carrageenans inhibit the *in vitro* growth of *Plasmodium falciparum* and cytoadhesion to CD36.** *Parasitol Res* 2005, **97**:290–294.
2. James MA, Alger NE: ***Plasmodium berghei*: effect of carrageenan on the course of infection in the A/J mouse.** *Int J Parasitol* 1981, **11**:217–220.
3. Moyana TN, Lalonde JM: **Carrageenan-induced intestinal injury in the rat –a model for inflammatory bowel disease.** *Ann Clin Lab Sci* 1990, **20**:420–426.
4. Merlo S, Dolovich J, Listgarten C: **Anaphylaxis to carrageenan: a pseudo-latex allergy.** *J Allergy Clin Immunol* 1995, **95**:933–936.
5. Tsuji RF, Hoshino K, Noro Y, Tsuji NM, Kurokawa T, Masuda T, Akira S, Nowak B: **Suppression of allergic reaction by λ-carrageenan: toll-like receptor 4/MyD88-dependent and -independent modulation of immunity.** *Clin Exp Allergy* 2003, **33**:249–258.
6. Tobacman JK, Wallace RB, Zimmerman MB: **Consumption of carrageenan and other water-soluble polymers used as food additives and incidence of mammary carcinoma.** *Med Hypotheses* 2001, **56**:589–598.
7. Silva FRF, Dore CMPG, Marques CT, Nascimento MS, Benevides NMB, Rocha HAO, Chavante SF, Leite EL: **Anticoagulant activity, paw edema and pleurisy induced carrageenan: action of major types of commercial carrageenans.** *Carbohydr Polym* 2010, **79**:26–33.
8. Suralkar AA, Sarda PS, Ghaisas MM, Thakare VN, Deshpande AD: **In-vivo animal models for evaluation of anti-inflammatory activity.** *Pharmainfonet* 2008, **6**: http://www.pharmainfo.net/reviews/vivo-animal-models-evaluation-anti-inflammatory-activity. Accessed July 8, 2014.
9. Huber JD, Hau VS, Borg L, Campos CR, Egleton RD, Davi TP: **Blood–brain barrier tight junctions are altered during a 72-h exposure to λ-carrageenan-induced inflammatory pain.** *Am J Physiol Heart Circ Physiol* 2002, **283**:H1531–H1537.
10. Rénia L, Howland SW, Claser C, Charlotte Gruner A, Suwanarusk R, Hui Teo T, Russel B, Ng LF: **Cerebral malaria: mysteries at the blood–brain barrier.** *Virulence* 2012, **3**:193–201.
11. Aikawa M, Iseki M, Barnwell JW, Taylor D, Oo MM, Howard RJ: **The pathology of cerebral malaria.** *Am J Trop Med Hyg* 1990, **43**:30–37.
12. van der Heyde HC, Nolan J, Combes V, Gramaglia I, Grau GE: **A unified hypothesis for the genesis of cerebral malaria: sequestration, inflammation and hemostasis leading to microcirculatory dysfunction.** *Trends Parasitol* 2006, **22**:503–508.
13. Ponsford MJ, Medana IM, Prapansilp P, Hien TT, Lee SJ, Dondorp AM, Esiri MM, Day NP, White NJ, Turner GD: **Sequestration and microvascular congestion are associated with coma in human cerebral malaria.** *J Infect Dis* 2012, **205**:663–671.
14. Jennings VM, Actor JK, Lal AA, Hunter RL: **Cytokine profile suggesting that murine cerebral malaria is an encephalitis.** *Infect Immun* 1997, **65**:4883–4887.
15. Bopp SER, Rodrigo E, Gonzalez-Paez GE, Frazer M, Barnes SW, Valim C, Watson J, Walker JR, Schemdt C, Winzeler EA: **Identification of the *Plasmodium berghei* resistance locus 9 linked to survival on chromosome 9.** *Malar J* 2013, **12**:316.
16. Carroll RW, Wainwright MS, Kim KY, Kidambi T, Gomez ND, Taylor T, Haldar K: **A rapid murine coma and behavior scale for quantitative assessment of murine cerebral malaria.** *PLoS One* 2010, **5**:e13124.
17. Nacer A, Movila A, Baer K, Mikolajczak SA, Kappe SHI, Frevert U: **Neuroimmunological blood brain barrier opening in experimental cerebral malaria.** *PLoS Pathog* 2012, **8**:e1002982. doi:10.1371/journal.ppat.1002982.
18. Schmidt KE, Schumak B, Specht S, Dubben B, Limmer A, Hoerauf A: **Induction of pro-inflammatory mediators in *Plasmodium berghei* infected BALB/c mice breaks blood–brain-barrier and leads to cerebral malaria in an IL-12 dependent manner.** *Microb Infect* 2011, **13**:828–836.
19. Taylor-Robinson AW: **Validity of modelling cerebral malaria in mice: argument and counter argument.** *J Neuroparasitol* 2010, **1**:N100601. doi:10.4303/jnp/N100601. Accessed July 8, 2014.
20. Bacchetti P, Deeks SG, McCune JM: **Breaking free of sample size dogma to perform innovative translational research.** *Sci Transl Med* 2011, **3**:87ps24.
21. Liu PT: **Extremely small sample size in some toxicity studies: an example from the rabbit eye irritation test.** *Regul Toxicol Pharmacol* 2001, **33**:187–191.
22. De Winter JCF: **Using the student's t-test with extremely small sample sizes.** *PARE* 2013, **18**:1–12.
23. Neill AL, Hunt NH: **Pathology of fatal and resolving *Plasmodium berghei* cerebral malaria in mice.** *Parasitology* 1992, **105**:165–175.
24. Huber JD, Campos CR, Mark KS, Davis TP: **Alterations in blood–brain barrier ICAM-1 expression and brain microglial activation after lambda-carrageenan-induced inflammatory pain.** *Am J Physiol Heart Circ Physiol* 2006, **290**:H732–H740.
25. Shear HL, Shear HL, Marino MW, Wanidworanun C, Berman JW, Nagel RL: **Correlation of increased expression of intercellular adhesion molecule-1, but not high levels of tumor necrosis factor-alpha, with lethality of *Plasmodium yoelii* 17XL, a rodent model of cerebral malaria.** *Am J Trop Med Hyg* 1998, **1998**(59):852–858.
26. Cserti-Gazdewich CM: ***Plasmodium falciparum* malaria and carbohydrate blood group evolution.** *ISBT Sci Ser* 2010, **5**:256–266. doi:10.1111/j.1751-2824.2010.01380.x.
27. Zhu HT, Bian C, Yuan JC, Chu WH, Xiang X, Chen F, Wang CS, Feng H, Lin JK: **Curcumin attenuates acute inflammatory injury by inhibiting the TLR4/MyD88/NF-κB signaling pathway in experimental traumatic brain injury.** *J Neuroinflammation* 2014, **11**:59. doi: 10.1186/1742-2094-11-59.
28. Clark DL, Su S, Davidson EA: **Saccharide anions as inhibitors of the malaria parasite.** *Glycoconj J* 1997, **14**:473–479.

29. Xiao L, Yang C, Patterson PS, Udhayakumar V, Lal AA: **Sulfated polyanions inhibit invasion of erythrocytes by *Plasmodium* merozoites and cytoadherence of endothelial cells to parasitized erythrocytes.** *Infect Immun* 1996, **64**:1373–1378.
30. Recuenco FC, Kobayashi K, Ishiwa A, Enomoto-Rogers Y, Fundador NGV, Sugi T, Takemae H, Iwanaga T, Murakoshi F, Gong H, Inomata A, Horimoto T, Iwata T, Kato K: **Gellan sulfate inhibits *Plasmodium falciparum* growth and invasion of red blood cells *in vitro*.** *Sci Rep* 2014, **4**:4723. doi:10.1038/srep04723.

doi:10.1186/1475-2875-13-487
Cite this article as: Recuenco *et al.*: Lambda-carrageenan treatment exacerbates the severity of cerebral malaria caused by *Plasmodium berghei* ANKA in BALB/c mice. *Malaria Journal* 2014 13:487.

Analytical Biochemistry 464 (2014) 9–11

Contents lists available at ScienceDirect

Analytical Biochemistry

journal homepage: www.elsevier.com/locate/yabio

Notes & Tips

Microplate assay for screening *Toxoplasma gondii* bradyzoite differentiation with DUAL luciferase assay

Tatsuki Sugi [a], Tatsunori Masatani [a,b], Fumi Murakoshi [a,c], Shin-ichiro Kawazu [a], Kentaro Kato [a,c,*]

[a] National Research Center for Protozoan Diseases, Obihiro University of Agriculture and Veterinary Medicine, Obihiro, Hokkaido 080-8555, Japan
[b] Transboundary Animal Diseases Center, Joint Faculty of Veterinary Medicine, Kagoshima University, Kagoshima 890-0065, Japan
[c] Department of Veterinary Microbiology, Graduate School of Agricultural and Life Sciences, University of Tokyo, Bunkyo-ku, Tokyo 113-8657, Japan

ARTICLE INFO

Article history:
Received 15 May 2014
Received in revised form 18 June 2014
Accepted 19 June 2014
Available online 30 June 2014

Keywords:
Bradyzoite
DUAL luciferase assay
High-throughput screening
Reporter parasite
Toxoplasma gondii

ABSTRACT

Toxoplasma gondii can differentiate into tachyzoites or bradyzoites. To accelerate the investigation of bradyzoite differentiation mechanisms, we constructed a reporter parasite, PLK/DLUC_1C9, for a high-throughput assay. PLK/DLUC_1C9 expressed firefly luciferase under the bradyzoite-specific BAG1 promoter. Firefly luciferase activity was detected with a minimum of 10^2 parasites induced by pH 8.1. To normalize bradyzoite differentiation, PLK/DLUC_1C9 expressed Renilla luciferase under the parasite's α-tubulin promoter. Renilla luciferase activity was detected with at least 10^2 parasites. By using PLK/DLUC_1C9 with this 96-well format screening system, we found that the protein kinase inhibitor analogs, bumped kinase inhibitors 1NM-PP1, 3MB-PP1, and 3BrB-PP1, had bradyzoite-inducing effects.

The infection prevalence of *Toxoplasma gondii*, a protozoan parasite in Apicomplexa, is high all over the world [1]. When *T. gondii* infects humans, it causes toxoplasmosis in infants [2] and immunocompromised patients [3]. *T. gondii* can differentiate into two types of cells in its intermediate host animals: a fast-replicating tachyzoite and a slow-replicating dormant bradyzoite in the cyst. Cell differentiation from tachyzoite to bradyzoite is related to infectious cyst formation in meat production animals (tachyzoite to bradyzoite) and to recurrence of latent infection in acquired immunodeficient patients (bradyzoite to tachyzoite) [4]. Bradyzoite-specific gene expression has been well documented via transcriptome analysis using *in vitro* systems [5] and *in vivo* cysts [6]. However, how the stress response is transduced and which signals lead to the transcriptional changes are not yet fully understood. To answer these questions, a high-throughput screening system to identify factors that affect bradyzoite differentiation would be a powerful tool.

A major requirement for bradyzoite differentiation screening is the availability of a robust, easy, and sensitive detection method. Moreover, normalization of bradyzoite-specific value with the parasite number is needed because bradyzoite-inducing conditions tend to influence the parasite growth itself [7]. A widely used assay for bradyzoite differentiation uses real-time quantitative reverse transcription polymerase chain reaction analysis of bradyzoite-specific gene expression with normalization by constitutively expressed tubulin messenger RNA levels [8]. Several groups have reported the transgenic parasite for investigating bradyzoite differentiation based on fluorescent reporter systems [9,10] and a luciferase assay system [5,11]. Several groups have reported transgenic parasites for investigating bradyzoite differentiation based on fluorescent reporter systems [9,10] and a luciferase assay system [5,11]. However, the fluorescent reporter systems lack sensitivity, and the luciferase assay lacks a normalization method unless transient transfection is employed before every assay.

In the current report, we describe a new reporter system, named pDUALUCI, that expresses firefly luciferase under the control of the bradyzoite-specific BAG1 [TGME49_259020] promoter as well as Renilla luciferase under the control of the constitutively expressed α-tubulin TUBA1 [TGME49_316400] promoter (Fig. 1A). Detailed plasmid construction information is provided in the online supplementary material. Host Vero cells and parasites were maintained as described elsewhere [12]. Plasmid DNA (20 μg) was linearized with *Not*I and transfected into 1.0×10^6 cells of the PLK/hxgprt$^-$ strain (National Institutes of Health AIDS Reagent Program, No. 2860) [12]; stable transgenic parasites were selected by 50 μg/ml mycophenolic acid and 50 μg/ml xanthine and were then cloned by limiting dilution as described elsewhere [13]. A parasite

* Corresponding author at: National Research Center for Protozoan Diseases, Obihiro University of Agriculture and Veterinary Medicine, Obihiro, Hokkaido 080-8555, Japan. Fax: +81 155 49 5646.
E-mail address: kkato@obihiro.ac.jp (K. Kato).

http://dx.doi.org/10.1016/j.ab.2014.06.018
0003-2697/

A

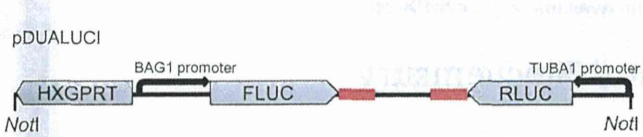

B

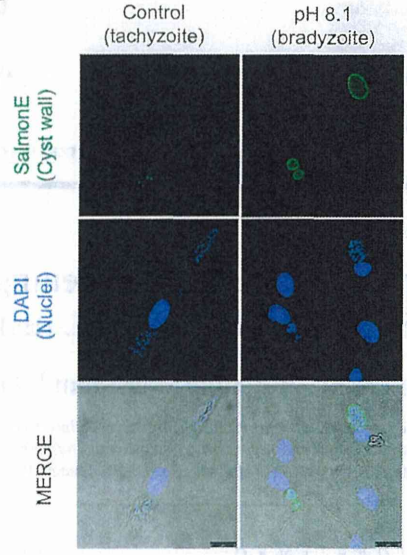

C

Detection range for the luciferase reporter activity

Condition	Cell number	Firefly Luciferase	Renilla luciferase
Tachyzoite	1.4E+05	2.7E+02 (±4.5E+00)	2.0E+06 (±3.3E+04)
	1.2E+04	N/D	2.1E+05 (±6.1E+03)
	1.1E+03	N/D	2.0E+04 (±7.3E+02)
	1.0E+02	N/D	1.8E+03 (±8.0E+01)
Bradyzoite	1.4E+05	8.1E+05 (±2.4E+04)	3.5E+06 (±4.4E+04)
	1.3E+04	8.2E+04 (±3.7E+03)	3.8E+05 (±1.3E+04)
	1.2E+03	7.8E+03 (±2.1E+02)	3.8E+04 (±1.9E+03)
	1.1E+02	7.3E+02 (±4.1E+01)	3.5E+03 (±1.5E+02)

Fig.1. Firefly luciferase expression by PLK/DLUC_1C9 is dependent on bradyzoite induction. (A) Schematic diagram of the DNA construct used to make PLK/DLUC_1C9. The *NotI sites used to linearize the plasmid are shown. Arrows show the directions of transcription. The diagram does not reflect the gene length. Red boxes show the terminator* sequence from 3′ UTR (untranslated region) of TgGRA2. (B) PLK/DLUC_1C9 can differentiate to bradyzoites. The cyst wall was stained with a SalmonE monoclonal antibody. Nuclei were stained with DAPI (4′,6-diamidino-2-phenylindole). The light fields combined with the fluorescent channels are shown as a merge. Scale bars = 25 μm. (C) Tachyzoites and bradyzoites were purified and counted by using a hemocytometer. The cell number denotes the parasite number in the lysate for the luciferase assay. Data are averages with standard deviations from three technical replicates. Values below the background average plus three times the background standard deviation are presented as N/D (not detected). (For interpretation of the reference to color in this figure legend, the reader is referred to the Web version of this article.)

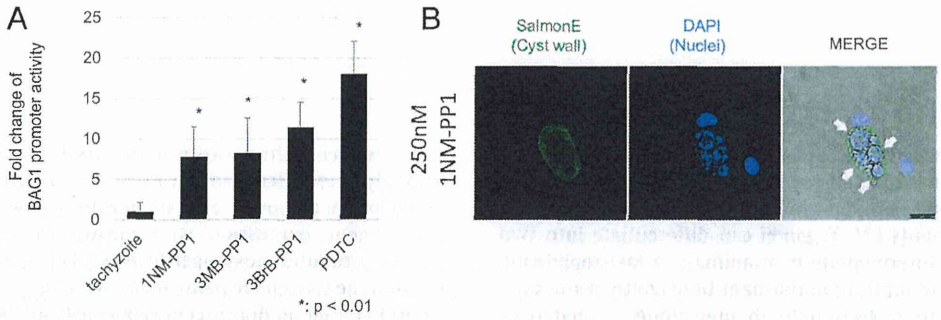

Fig.2. A 96-well microplate assay for bradyzoite differentiation. (A) 80 μM PDTC; 250 nM 1NM-PP1, 3MB-PP1, and 3BrB-PP1; and control medium containing dimethyl sulfoxide (final 0.1%, v/v) were used for the parasite treatment. BAG1 promoter activity was calculated by dividing the firefly luciferase activity by the Renilla luciferase activity. Fold changes in the bradyzoite promoter activity from the control sample are shown. Error bars show the standard deviations from independent quadruplicate experiments. An asterisk (*) indicates a *P* value < 0.01 by Student *t* test between the treatment and tachyzoite control. (B) 1NM-PP1 (250 nM) induces cyst wall formation and inhibits normal parasite growth. HFF cells infected by PLK/DLUC_1C9 were treated with 250 nM 1NM-PP1 from 2 h after parasite inoculation for 4 days. The cyst wall was stained with SalmonE monoclonal antibody. Nuclei were stained with DAPI (4′,6-diamidino-2-phenylindole). The light field and the fluorescent channels are shown as a merge. Scale bars = 25 μm. Arrows show the abnormally large cells in the parasitophorous vacuole.

clone, which exhibited the highest luciferase luminescence, was designated as PLK/DLUC_1C9. To determine whether PLK/DLUC_1C9 could differentiate to bradyzoites, we observed cyst wall formation. Human foreskin fibroblast (HFF)[1] cells were maintained as described elsewhere [12]. For bradyzoite induction, PLK/DLUC_1C9-infected HFF cells were treated with 1% fetal calf serum in Dulbecco's modified Eagle's medium with 25 mM Hepes (pH 8.1) without $NaHCO_3$ from 2 h after parasite inoculation and were incubated in humid air for 4 days. The cells were then fixed with 4% paraformaldehyde and stained with an anti-CST1 SalmonE monoclonal antibody as described elsewhere [14]. The pH 8.1 medium-treated PLK/DLUC_1C9 showed cyst wall staining, whereas the tachyzoite control showed no staining in the parasitophorous vacuole membranes (Fig. 1B). To measure the detection limit of the luciferase assay, we measured the luciferase activity of purified parasites. Parasite pellets were lysed in Passive Lysis Buffer (Promega) and used in the luciferase assay according to the instructions provided by the manufacturer of the Dual-Luciferase Reporter Assay System (Promega) using LUMAT LB9507 (Berthold). The background luminescence value from the lysis buffer containing no parasites was subtracted from the raw values and estimated to give relative luminescence values. We found that 1.1×10^2 parasites were sufficient to

[1] *Abbreviations used:* HFF, human foreskin fibroblast; PDTC, pyrrolidinedithiocarbamate; BKI, bumped kinase inhibitor.

detect the firefly luciferase activity in the bradyzoites (Fig. 1C). Renilla luciferase activity was detected with a minimum of 1.0×10^2 tachyzoites and 1.1×10^2 bradyzoites (Fig. 1C).

Next, we tested PLK/DLUC_1C9 in the microplate format assay. We tested 80 μM ammonium pyrrolidinedithiocarbamate (PDTC, Sigma–Aldrich) as a known bradyzoite-inducing agent [5]. The microplate assay was performed as described in Supplemental Fig. 2. The 80-μM PDTC treatment increased the BAG1 promoter activity by 18-fold when compared with the tachyzoite control (Fig. 2A). We also tested bumped kinase inhibitors (BKIs), which have few sensitive protein kinases in mammalian genome [15] and for which *in vivo* effects have been reported in a mouse infection model [16–18]. TgMAPK1 is a secondary target of BKIs [19], and its involvement in bradyzoite differentiation [20] and cell division [19] has been reported. Three commercial BKIs induced BAG1 promoter activity by approximately 8- to 11-fold (Fig. 2A) when compared with the normal tachyzoite culture conditions (7.8-fold, 1NM-PP1 [Merck]; 8.2-fold, 3MB-PP1 [Toronto Research Chemicals, TRC]); 11-fold, 3BrB-PP1 [TRC]). Accompanying the up-regulation of BAG1 promoter activity, 1NM-PP1-treated parasites formed cyst walls and appeared abnormally large in the parasitophorous vacuoles (Fig. 2B). This large parasite was also reported as an effect to *Neospora caninum* when the parasite was treated with bumped kinase inhibitor 1294 [21]. Therefore, PLK/DLUC_1C9 could detect the BAG1 promoter activation from the induction of cyst genesis by 1NM-PP1.

In summary, our data show that PLK/DLUC_1C9 provides an alternative method for evaluating bradyzoite induction levels in a microplate assay format with normalization via TUBA1 promoter activity and will be of value in revealing the factors affecting bradyzoite differentiation.

Acknowledgments

PLK/hxgprt$^-$ was obtained through the AIDS Reagent Program, Division of AIDS, National Institute of Allergies and Infectious Diseases (NIAID), National Institutes of Health (NIH), from David Roos. SalmonE monoclonal antibody was a kind gift from Louis M. Weiss. We thank T. Tomita for technical advice regarding cyst wall staining. T.S. and F.M. were supported by a Japan Society for the Promotion of Science (JSPS) Research Fellowship for Young Scientists. K.K. was supported by Grants-in-Aid for Young Scientists, Exploratory Research, Scientific Research on Innovative Areas (3308) from the Ministry of Education, Culture, Science, Sports, and Technology (MEXT) of Japan, the Program for the Promotion of Basic and Applied Research for Innovations in Bio-oriented Industry (BRAIN), the Science and Technology Research Promotion Program for Agriculture, Forestry, Fisheries, and Food Industry, and the Program to Disseminate Tenure Tracking System from the Japan Science and Technology Agency (JST). T.M. was supported by JSPS KAKENHI grants (24780295 and 26850183).

Appendix A. Supplementary data

Supplementary data associated with this article can be found, in the online version, at http://dx.doi.org/10.1016/j.ab.2014.06.018.

References

[1] G. Pappas, N. Roussos, M.E. Falagas, Toxoplasmosis snapshots: global status of *Toxoplasma gondii* seroprevalence and implications for pregnancy and congenital toxoplasmosis, Int. J. Parasitol. 39 (2009) 1385–1394.
[2] Y. Carlier, C. Truyens, P. Deloron, F. Peyron, Congenital parasitic infections: a review, Acta Trop. 121 (2012) 55–70.
[3] M.W. Wulf, R. van Crevel, R. Portier, C.G. ter Meulen, W.J. Melchers, A. van der Ven, J.M. Galama, Toxoplasmosis after renal transplantation: implications of a missed diagnosis, J. Clin. Microbiol. 43 (2005) 3544–3547.
[4] M.W. Black, J.C. Boothroyd, Lytic cycle of *Toxoplasma gondii*, Microbiol. Mol. Biol. Rev. 64 (2000) 607–623.
[5] M.S. Behnke, J.B. Radke, A.T. Smith, W.J. Sullivan, M.W. White, The transcription of bradyzoite genes in *Toxoplasma gondii* is controlled by autonomous promoter elements, Mol. Microbiol. 68 (2008) 1502–1518.
[6] K.R. Buchholz, H.M. Fritz, X. Chen, B. Durbin-Johnson, D.M. Rocke, D.J. Ferguson, P.A. Conrad, J.C. Boothroyd, Identification of tissue cyst wall components by transcriptome analysis of in vivo and in vitro *Toxoplasma gondii* bradyzoites, Eukaryot. Cell 10 (2011) 1637–1647.
[7] M.F. Ferreira da Silva, H. Barbosa, U. Gross, C. Lüder, Stress-related and spontaneous stage differentiation of *Toxoplasma gondii*, Mol. Biosyst. 4 (2008) 824–834.
[8] J. Narasimhan, B.R. Joyce, A. Naguleswaran, A.T. Smith, M.R. Livingston, S.E. Dixon, I. Coppens, R.C. Wek, W.J. Sullivan, Translation regulation by eukaryotic initiation factor-2 kinases in the development of latent cysts in *Toxoplasma gondii*, J. Biol. Chem. 283 (2008) 16591–16601.
[9] A. Unno, K. Suzuki, T. Batanova, S. Cha, H. Jang, K. Kitoh, Y. Takashima, Visualization of *Toxoplasma gondii* stage conversion by expression of stage-specific dual fluorescent proteins, Parasitology 136 (2009) 579–588.
[10] H. Zhang, Y. Zhang, J. Cao, Y. Zhou, N. Wang, J. Zhou, Determination of stage interconversion *in vitro* and *in vivo* by construction of transgenic *Toxoplasma gondii* that stably express stage-specific fluorescent proteins, Exp. Parasitol. 134 (2013) 275–280.
[11] M. Di Cristina, D. Marocco, R. Galizi, C. Proietti, R. Spaccapelo, A. Crisanti, Temporal and spatial distribution of *Toxoplasma gondii* differentiation into bradyzoites and tissue cyst formation *in vivo*, Infect. Immun. 76 (2008) 3491–3501.
[12] D.S. Roos, R.G. Donald, N.S. Morrissette, A.L. Moulton, Molecular tools for genetic dissection of the protozoan parasite *Toxoplasma gondii*, Methods Cell Biol. 45 (1994) 27–63.
[13] T. Sugi, K. Kato, K. Kobayashi, S. Watanabe, H. Kurokawa, H. Gong, K. Pandey, H. Takemae, H. Akashi, Use of the kinase inhibitor analog 1NM-PP1 reveals a role for *Toxoplasma gondii* CDPK1 in the invasion step, Eukaryot. Cell 9 (2010) 667–670.
[14] T. Tomita, D.J. Bzik, Y.F. Ma, B.A. Fox, L.M. Markillie, R.C. Taylor, K. Kim, L.M. Weiss, The *Toxoplasma gondii* cyst wall protein CST1 is critical for cyst wall integrity and promotes bradyzoite persistence, PLoS Pathog. 9 (2013) e1003823.
[15] K.K. Ojo, R.T. Eastman, R. Vidadala, Z. Zhang, K.L. Rivas, R. Choi, J.D. Lutz, M.C. Reid, A.M. Fox, M.A. Hulverson, M. Kennedy, N. Isoherranen, L.M. Kim, K.M. Comess, D.J. Kempf, C.L. Verlinde, X.Z. Su, S.H. Kappe, D.J. Maly, E. Fan, W.C. Van Voorhis, A specific inhibitor of *Pf*CDPK4 blocks malaria transmission: chemical–genetic validation, J. Infect. Dis. 209 (2014) 275–284.
[16] T. Sugi, K. Kato, K. Kobayashi, H. Kurokawa, H. Takemae, G. Haiyan, F.C. Recuenco, T. Iwanaga, T. Horimoto, H. Akashi, 1NM-PP1 treatment of mice infected with *Toxoplasma gondii*, J. Vet. Med. Sci. 73 (2011) 1377–1379.
[17] S. Lourido, C. Zhang, M.S. Lopez, K. Tang, J. Barks, Q. Wang, S.A. Wildman, K.M. Shokat, L.D. Sibley, Optimizing small molecule inhibitors of calcium-dependent protein kinase 1 to prevent infection by *Toxoplasma gondii*, J. Med. Chem. 56 (2013) 3068–3077.
[18] J.S. Doggett, K.K. Ojo, E. Fan, D.J. Maly, W.C. Van Voorhis, Bumped kinase inhibitor 1294 treats established *Toxoplasma gondii* infection, Antimicrob. Agents Chemother. 58 (2014) 3547–3549.
[19] T. Sugi, K. Kobayashi, H. Takemae, H. Gong, A. Ishiwa, F. Murakoshi, F.C. Recuenco, T. Iwanaga, T. Horimoto, H. Akashi, K. Kato, Identification of mutations in TgMAPK1 of *Toxoplasma gondii* conferring resistance to 1NM-PP1, Int. J. Parasitol. Drugs Drug Resist. 3 (2013) 93–101.
[20] M.J. Brumlik, S. Wei, K. Finstad, J. Nesbit, L.E. Hyman, M. Lacey, M.E. Burow, T.J. Curiel, Identification of a novel mitogen-activated protein kinase in *Toxoplasma gondii*, Int. J. Parasitol. 34 (2004) 1245–1254.
[21] K.K. Ojo, M.C. Reid, L. Kallur Siddaramaiah, J. Müller, P. Winzer, Z. Zhang, K.R. Keyloun, R.S. Vidadala, E.A. Merritt, W.G. Hol, D.J. Maly, E. Fan, W.C. Van Voorhis, A. Hemphill, Neospora caninum calcium-dependent protein kinase 1 is an effective drug target for neosporosis therapy, PLoS One 9 (2014) e92929.